

1 Technical Note: Noble gas extraction procedure and performance of the
2 Cologne Helix MC Plus multi-collector noble gas mass spectrometer for
3 cosmogenic neon isotope analysis

4 Benedikt Ritter^{1*}, Andreas Vogt¹, Tibor J. Dunai^{1*}

5 ¹ University of Cologne, Institute of Geology and Mineralogy, Zùlpicher StraÙe 49b, Köln 50674,
6 Germany

7 *Corresponding authors

8 Benedikt Ritter – benedikt.ritter@uni-koeln.de

9 Tibor J. Dunai – tdunai@uni-koeln.de

10 Keywords: Noble Gas, Mass Spectrometry, Cosmogenic Nuclides

11
12 **Abstract:**

13 We established a new laboratory for noble gas mass spectrometry that is dedicated to the
14 development and application to cosmogenic nuclides at the University of Cologne (Germany). At
15 the core of the laboratory are a state-of-the-art high mass resolution multicollector Helix MCPlus
16 (Thermo-Fisher) noble gas mass spectrometer and a novel custom-designed automated
17 extraction line. The mass spectrometer is equipped with five combined Faraday Multiplier
18 collectors, with $10^{12} \Omega$ and $10^{13} \Omega$ pre-amplifiers for faraday collectors. We describe the extraction
19 line and the automated procedure for cosmogenic neon and the current performance of the
20 experimental setup. Performance tests were conducted using gas of atmospheric isotopic
21 composition (our primary standard gas), as well as CREU-1 intercomparison material, containing
22 a mixture of neon of atmospheric and cosmogenic composition. We use the results from repeated
23 analysis of CREU-1 to assess the performance of the current experimental setup at Cologne. The
24 precision in determining the abundance of cosmogenic ^{21}Ne is equal to or better than those
25 reported for other laboratories. The absolute value we obtain for the concentration of cosmogenic
26 ^{21}Ne in CREU is indistinguishable from the published value.

27 **1. Introduction**

28 Cosmogenic Ne isotopes are stable and compared to other cosmogenic radionuclides (e.g., ^{10}Be ,
29 ^{26}Al) exhibit the potential to date beyond the physical limit of radionuclides. The particular
30 strength of cosmogenic neon is its application to date quartz clasts of very old surfaces (>4 Ma) or
31 very slowly eroding landscapes (<10 cm/Ma), which is unattainable with most other
32 radionuclides (Dunai, 2010). Cosmogenic Ne analysis can be applied to a range of neon-retentive
33 minerals (e.g., quartz, olivine and pyroxene), amongst which quartz is the most commonly used.
34 Ne can be measured on conventional sector field noble gas mass spectrometers, is less time
35 consuming and requires less sample-preparation compared to AMS measurements required for

36 the cosmogenic radionuclides. Recent studies used cosmogenic Ne for dating old surfaces (e.g.
37 Ritter et al., 2018; Dunai et al., 2005; Binnie et al., 2020), reconstructing erosion rates (e.g. Ma et
38 al., 2016), or $^{10}\text{Be}/^{21}\text{Ne}$ burial dating (e.g. McPhillips et al., 2016). The advantage to use also other
39 minerals than quartz, led to several studies using ^{21}Ne to date for example basalt flows (e.g.
40 Espanon et al., 2014; Gillen et al., 2010). Neon has three stable isotopes ^{20}Ne , ^{21}Ne , and ^{22}Ne , of
41 which ^{20}Ne is the most abundant; the atmospheric $^{21}\text{Ne}/^{20}\text{Ne}$ and $^{22}\text{Ne}/^{20}\text{Ne}$ ratios are $0.002959 \pm$
42 0.000022 and 0.1020 ± 0.0008 , respectively (Eberhardt et al., 1965). There are several recent
43 re-determinations of the atmospheric $^{21}\text{Ne}/^{20}\text{Ne}$ ratio (e.g. Honda et al., 2015; Wielandt and
44 Storey, 2019; Saxton, 2020; Györe et al., 2019) one of which yields a $\sim 2\%$ lower value (Honda et
45 al., 2015). For the evaluation of our data, we utilize the $^{21}\text{Ne}/^{20}\text{Ne}$ value of Wielandt and Storey
46 (2019) of 0.0029577 ± 0.0000014 and for $^{22}\text{Ne}/^{20}\text{Ne}$ that of Eberhardt et al. (1965). Note, that in
47 the context of the determination of the *abundance* of cosmogenic nuclides in a sample eventual
48 differences between the used and the actual value of the atmospheric $^{21}\text{Ne}/^{20}\text{Ne}$ ratio are
49 unimportant, if (i) atmospheric neon is used as calibration gas, (ii) the same value for the
50 composition of atmospheric neon is used consistently throughout the evaluation of the isotope
51 data (mass discrimination etc.) and calculation of abundances and (iii) the atmospheric value used
52 is reported along with the data.

53 All three neon isotopes are produced in about equal proportions by neutron spallation in quartz
54 (Niedermann et al., 1994). Due to the lower abundances of ^{21}Ne and ^{22}Ne as compared to ^{20}Ne in
55 air, and the ubiquitous presence of atmospheric neon in samples, any contribution from
56 cosmogenic production in samples is most easily picked up with the former two isotopes.
57 Consequently, the neon three-isotope diagram with ^{20}Ne as common denominator (Niedermann
58 et al., 1994; Niedermann, 2002) is customarily used to assess ^{21}Ne -data for the presence of
59 terrestrial cosmogenic Ne and its discrimination from other non-atmospheric Ne-components
60 (Dunai, 2010). The latter may be nucleonic Ne and/or mantle-derived Ne. Hence, the accurate
61 determination of cosmogenic Ne and its discrimination from other components requires the
62 accurate discrimination from any other component.

63 **Common isobaric interferences for neon measurements are at: $m/e = 20$ ($^{40}\text{Ar}^{2+}$, H^{19}F^+ and $\text{H}_2^{18}\text{O}^+$
64 **interfering with $^{20}\text{Ne}^+$), at $m/e = 21$ ($^{20}\text{NeH}^+$, interfering with $^{21}\text{Ne}^+$), and at $m/e = 22$ ($^{44}\text{CO}_2^{2+}$
65 **interfering with $^{22}\text{Ne}^+$).** $^{40}\text{Ar}^{2+}$ and $^{12}\text{C}^{16}\text{O}_2^{2+}$ interferences are considered to be the main challenges
66 for neon analysis. Recent studies demonstrated the ability of the Helix MCPlus to fully resolve the
67 $^{40}\text{Ar}^{2+}$, H^{19}F^+ and $\text{H}_2^{18}\text{O}^+$ peaks from the $^{20}\text{Ne}^+$ peak (e.g. Honda et al., 2015; Wielandt and Storey,
68 2019) and its ability to reliably measure ^{21}Ne at an off-centre peak position that is free of
69 interference from $^{20}\text{NeH}^+$ (Honda et al., 2015; Wielandt and Storey, 2019). The remaining
70 interference of $^{12}\text{C}^{16}\text{O}_2^{2+}$ at $m/e = 22$ can be corrected via monitoring of the double/single-charged
71 ratio of CO_2 in-between samples (Honda et al., 2015) or the measurement of $^{13}\text{C}^{16}\text{O}_2^{2+}$ at****

72 m/e = 22.5 during sample analysis (Wielandt and Storey, 2019). Recently mass spectrometers
73 with higher resolution have become available, which permit almost full separation of $^{12}\text{C}^{16}\text{O}_2^{2+}$ and
74 ^{22}Ne (Farley et al., 2020).

75 Beside the resolution and characteristics of a noble gas mass spectrometer to resolve and
76 quantitatively determine neon compositions of an unknown sample, the calibration, sample
77 extraction and purification are crucial achieving accurate and reproducible results. Automation of
78 extraction protocols and workflows may assist in achieving a high degree of reproducibility by
79 eliminating inaccuracies or errors by operators having a variable degree of expertise. In this
80 paper, we describe the current setup of the noble gas mass spectrometer and its automated
81 extraction line that is located in the Institute of Geology and Mineralogy at the University of
82 Cologne (Germany), and we review its performance for neon analysis.

83 **2. Experimental setup**

84 **2.1 Noble gas mass-spectrometer**

85 The Cologne noble gas laboratory is equipped with a Helix MCPlus from Thermo Fisher Scientific
86 with five CFM modules (Combined Faraday Multiplier), called 'Aura'. The central, axial module
87 (Ax) is fixed in position, the four remaining modules (L1, L2 on the low mass side, and H1,
88 H2 on the high mass side of Ax) can be moved. The mass spectrometer configuration and
89 performance is mostly equivalent to those described elsewhere (Honda et al., 2015; Wielandt and
90 Storey, 2019); here we describe potential differences in configuration and performance
91 parameters that may be unique to a given instrument (Fig. 1).

92 In the instrument at Cologne University, all but one Faraday amplifier, are equipped with $10^{13} \Omega$
93 resistors, one with $10^{12} \Omega$ (H2). The L1 module has 0.3 mm wide collector slits, all other modules
94 have 0.6 mm wide slits. The CFM at L1 configuration is flipped (i.e., the relative positions of the
95 Faraday and Multiplier are swapped) as compared to the standard configuration, which is the only
96 difference from the standard configuration. The two SAES NP10 getters, at the source and the
97 multiplier block, are kept at room temperature during analysis.

98 For neon isotope analysis of calibrations and samples, we utilize the H1, Ax and L1 CFMs ($^{20}\text{Ne}^+$
99 L1 Faraday; $^{22}\text{Ne}^+$ H1 Faraday; $^{21}\text{Ne}^+$ L1 multiplier; CO_2^+ H1 Faraday; for blanks we utilize the L1
100 multiplier also for $^{20}\text{Ne}^+$ and $^{22}\text{Ne}^{++}$). With the widest source slit (0.25 mm) mass resolution (at 5%
101 peak valley) and mass resolving power (between 10% and 90% of peak) on the L1 detector with
102 0.3 mm collector slit width are approximately 1700 and 6500, respectively. For the Ax and H1
103 detectors with 0.6 mm collector slit, the corresponding values are approximately 1000 and 6000,
104 respectively. As such the system allows the interference-free determination of ^{20}Ne and ^{21}Ne ; for

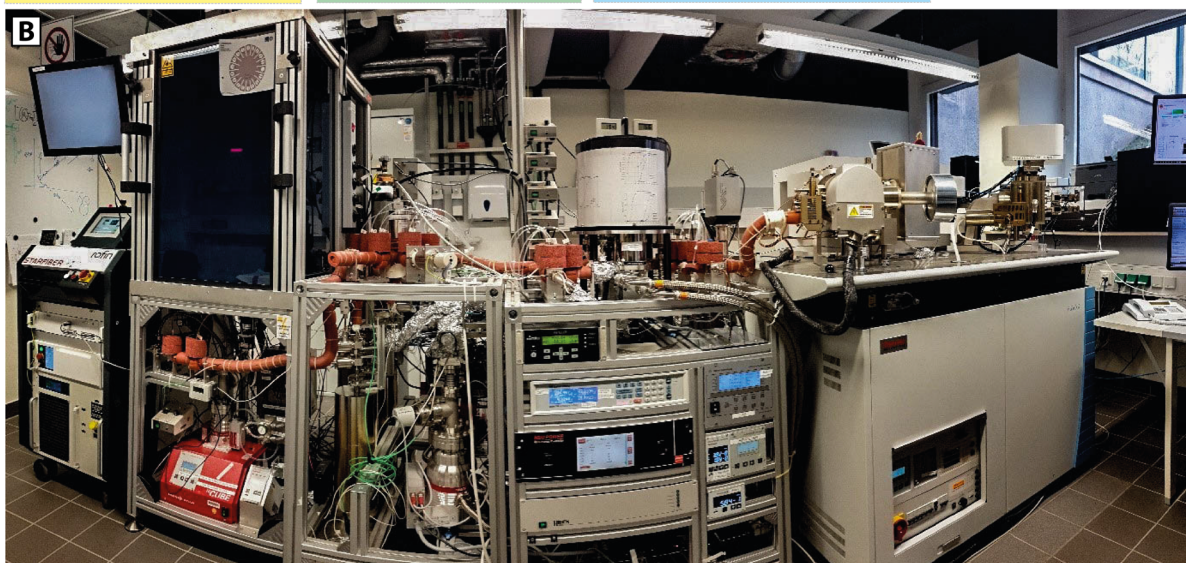
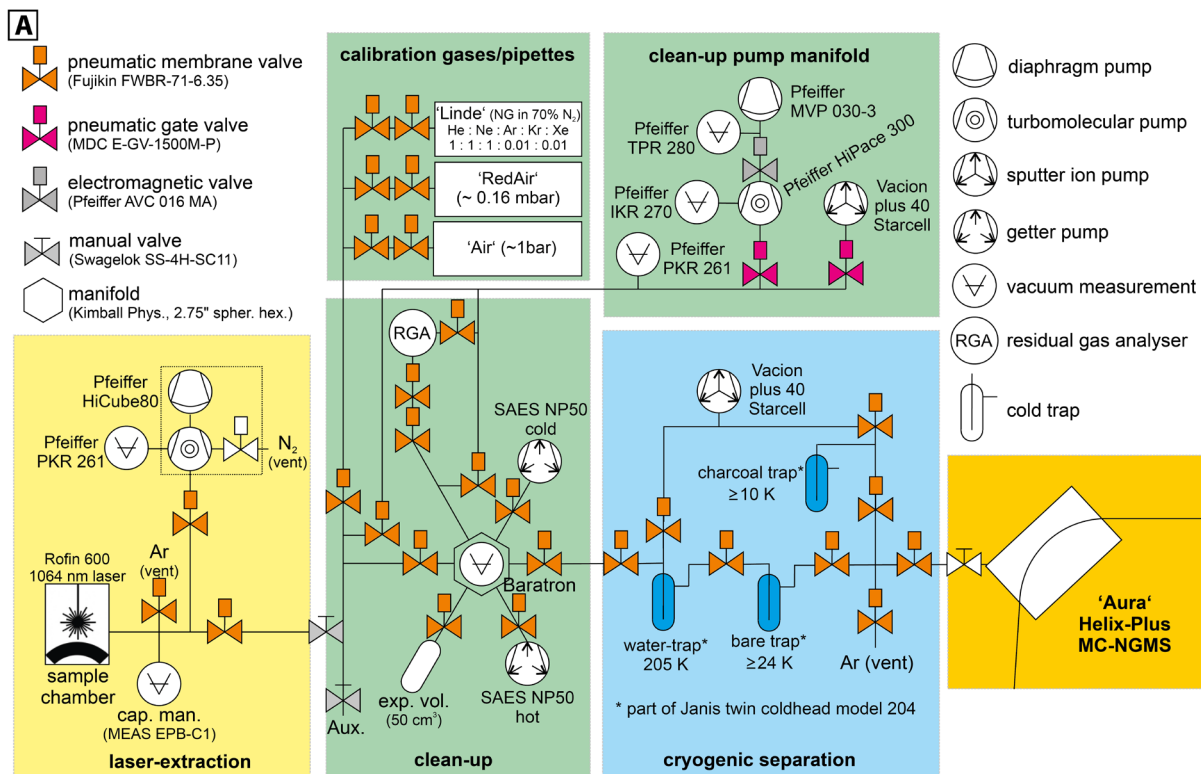
105 ^{21}Ne this entails measuring at an off-centre peak position (Honda et al., 2015; Wielandt and Storey,
106 2019).

107 **2.2 Extraction line**

108 The **Cologne** noble gas extraction and purification line has a modular design. Modules are (i)
109 extraction (currently only laser extraction; to be joined by a crushing device), (ii) calibration gas
110 pipettes and volumes, (iii) clean-up, and (iv) cryogenic separation. The calibration module is
111 physically linked to the clean-up module, the other modules can be separated, if required. Among
112 the common features of all modules is that all valves and tubing in contact with the sample gas are
113 made of metal; tubing is of stainless steel or vacuum-annealed copper. Furthermore, all valves
114 used for handling of sample and calibration gas are pneumatically actuated all-metal diaphragm
115 valves (Fujikin MEGA-M LA; FWB(R)-71-6.35), that can be operated at high temperature (up to
116 350°C). Tubing and valves in contact with sample gas are continuously kept at constant
117 temperature between 160 °C and 200 °C; exceptions are the functional traps and portions of the
118 tubing in the cryogenic separation. Temperature is maintained with heating tapes (Horst HS
119 450 °C) and is controlled section-wise (Horst HT30). The temperature of the heated sections is
120 controlled to ± 1 °C. Thermal insulation is achieved with high-temperature resistant silicone foam
121 (HOKOSIL®; resists ≤ 280 °C; permitting bake-out at higher than operation temperatures).
122 Vacuum connections used are VCR (for Fujikin Valves), CF (for adapters, getters and manifold in
123 clean up) and Swagelok (for flexible tubing between modules and between ports of the cryogenic
124 separator (Swagelok 321 Stainless Steel Flexible Tubing with XBA adapter; and copper tubing).
125 Tubing and valves are 1/4" outer diameter (Swagelok) or equivalent (VCR, Fujikin). The overall
126 internal volume of the extraction line (laser-extraction, clean-up & cryogenic separation) is
127 530 cm³. Outside the volume used for sample preparation, CF connections are used throughout. A
128 schematic overview and picture of the extraction line is provided in Figure 1.

129

130



131

132 *Fig. 1: (A) Schematic plan and picture (B) of the noble gas extraction and purification line at the*
 133 *University of Cologne. From left to right: Rofin Starfiber 600, full-protection laser-cage (laser*
 134 *protection windows P1P10, Laservision) housing the laser extraction, clean up unit, cryogenic*
 135 *separation unit and the Helix Plus NG-MCMS 'Aura'. The laboratory is temperature-stabilized to*
 136 *±0.5 °C. Further description is provided in the text.*

137 More specifically about the individual modules:

- 138 i. **Laser extraction module: Up to eighteen tungsten cups are loaded in a sample revolver, housed**
 139 **in a DN 200 CF flange-sandwich. The sample revolver is machined from molybdenum, which**
 140 **permits the heating of the tungsten cups while being situated in the revolver. To minimize**

141 heat-loss through conduction, the cups sit on shards of zirconia (synthetic, cubic-stabilized
142 ZrO_2). The tungsten cups can hold up to ~600 mg quartz. The tungsten cups are reused. When
143 analysing quartz, tungsten cups are emptied with a suction micropicker (Micropicker MPC100;
144 VU Amsterdam), while remaining in the sample revolver. In cases where samples are melted
145 during extraction, tungsten cups could be cleaned in HF (then of course outside the revolver).
146 For sample loading the volume containing the revolver is vented and continuously flushed with
147 high-purity nitrogen. During laser extraction the pressure is monitored (MEAS EPB-C1 sensor,
148 welded into a male VCR connector; Disynet), in case of an eventual failure of the viewport, the
149 extraction volume is automatically purged with Argon. Energy for the heat-extraction is
150 provided by an output-tuneable 600 W fiberlaser (Rofin StarFiber600) at 1064 nm wavelength
151 through galvanometer scanner optics (Rofin RS S 14 163/67 0°) and a sapphire viewport (Kurt
152 Lesker, VPZL-275DUS). For neon-extraction of quartz, the cups are covered with tungsten-lids;
153 the heating occurs via scanning of the lids (scanning speed 20 cm/s; rastering a circular area
154 of 10 mm diameter) with a defocused (~ 0.5 mm diameter) continuous wave beam with
155 100 W power for 15 min. Copper (melting point 1085 °C), placed in the cup-assemblies, melts
156 at 80 W laser power (15 min extraction time); we assume that at 100 W laser power the
157 internal temperature is ≥ 1200 °C. The temperature of the top of the tungsten lids is monitored
158 with a pyrometer (CellaTemp PA 29 AF 2/L; Keller HCW). The laser extraction has a dedicated
159 pumping unit (Pfeiffer HiCube80). Pressures attained after sample loading and heating of the
160 revolver (via short-term laser-heating – stepwise increased to 200 W - of an empty tungsten
161 cup; the external housing flanges reach ~50 °C during this treatment; temperatures in adjacent
162 cups in the revolver stay below 156.6° C, which was verified with Indium wire) are usually
163 $< 5 \cdot 10^{-9}$ mbar (the lower limit of the pressure gauge used) after one night of pumping. Typical
164 blanks, obtained via heating of an empty tungsten cup assembly, are ~0.3 fmol Neon. A detailed
165 description of this novel laser-furnace will be provided elsewhere.

166 ii. Calibration gas pipette module: The gas-pipettes are assemblies of male and female versions
167 of pneumatically actuated Fujikin diaphragm valves (MEGA-M LA; FWB(R)-71-6.35); the
168 reservoirs were manufactured by Caburn-MDC, the insides of the reservoirs are
169 electropolished. We currently have three different gases available for noble gas calibration
170 ('Linde', 'Air', 'RedAir'). 'Linde' is a noble gas mixture in nitrogen ($9.889 \pm 0.009\%$ He,
171 $10.00 \pm 0.01\%$ Ne, $10.01 \pm 0.01\%$ Ar, $0.00987 \pm 0.0003\%$ Kr; $0.01023 \pm 0.00002\%$ Xe; all
172 uncertainties are $\pm 2\sigma$; remainder N_2 , prepared gravimetrically by Linde; values as certified by
173 Linde according to DIN ISO 6141) the He is enriched in 3He ($12.3 \pm 0.3 R_a$; $\pm 2\sigma$; value as certified
174 by Linde according to DIN ISO 6141), the remaining noble gases have atmospheric
175 composition. We assume that the cryogenically purified atmospheric gases used by Linde were
176 not fractionated during this process; we have verified this for Ne within the limits of

177 uncertainties reported in this paper. 'Air' is a reservoir of air at atmospheric pressure and
178 'RedAir' a reservoir of air at reduced pressure (lab-name 'RedAir' is the abbreviation of that
179 fact). For the neon determinations we utilize 'RedAir'. The volumes of all reservoirs and the
180 pipettes have been determined relative to a gravimetrically calibrated gas volume (an
181 assembly of a Swagelok SS-4H valve and a Swagelok SS-4CS-TW-50 miniature cylinder;
182 repeatedly weighed (Satorius MSA524P-1000-DI; the balance was calibrated prior to
183 calibration of the reference volume) under vacuum and filled with air at a temperature (n=16),
184 pressure and relative humidity measured with traceable and/or certified sensors
185 (thermometer: testo 110; manometer: Greisinger GMH 3181-12, DKD certificate D19853, D-K-
186 15070-01-01; hygrometer: VWR traceable 628-0031); reference volume is $51.37 \pm 0.18 \text{ cm}^3$
187 ($\pm 1\sigma$). All other volumes (piping of the calibration gas filling line; pipettes and reservoirs) were
188 determined by taking pressure readings (MKS Baratron, Type 628FU5TCF1B) from repeated
189 step-wise expansion of gases. The temperature in the room where these calibrations were
190 conducted was stable to $\pm 0.5 \text{ }^\circ\text{C}$ over the course of the calibrations. The thus determined
191 volumes of the reservoir and pipette of 'RedAir' are $8740 \pm 35 \text{ cm}^3$ and $1.457 \pm 0.006 \text{ cm}^3$ ($\pm 1\sigma$),
192 respectively. For filling of the 'RedAir' reservoir one pipette volume of air was expanded into
193 the reservoir; the temperature, pressure and humidity at the time of filling of the pipette were
194 measured with a traceable and certified sensor (same as above). The first pipette volume
195 extracted from the 'RedAir' reservoir contained $4.020 \pm 0.027 \times 10^{-9} \text{ cm}^3$ ($\pm 1\sigma$) atmospheric
196 neon at standard temperature and pressure ($179 \pm 1 \text{ fmol}$ atmospheric neon; $\pm 1\sigma$).

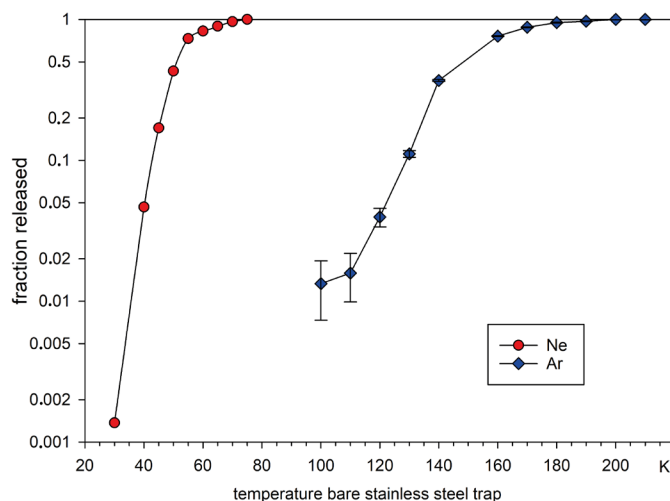
197 iii. Clean-up module ('Sputnik', lab-name, referring to the shape and protrusions of the central
198 manifold and its faint resemblance to the first satellite). Arranged around a central hexagonal
199 8-port manifold (Kimball Physics, 2.75" spherical hexagon) are the sample/calibration inlet,
200 the pumping outlet, a pipette leading to a residual gas analyser (Hiden HAL/3F PIC), two SAES
201 NP50 getters (one operated hot; heating current 1.6 A; $\sim 300 \text{ }^\circ\text{C}$), the other at room
202 temperature; getters are housed in SAES GP 50 W2F bodies; water cooling is optional, not used
203 during sample analysis), an optional expansion volume, an internally heated capacitance
204 manometer (MKS Baratron, Type 628FU5TCF1B; @ 100°C) and the outlet to the cryogenic
205 separation unit (Fig. 1). The sample/calibration inlet tubing has an auxiliary port, which e.g., is
206 used for the crushing extraction module (build around a T4S crushing unit, VU Amsterdam).
207 The clean-up module is pumped via a manifold connected through gate-valves (MDC E-GV-
208 1500M-P) to a turbopump (Pfeiffer HiPace 300; backed by a membrane pump, Pfeiffer MVP
209 030-3) and an ion pump (Agilent, Vacion 40 plus Starcell).

210 iv. Cryogenic separation module: Centre of this module is a double-cold trap unit (Janis, twin
211 coldhead model 204) that has inlet and outlet lines to three traps: a watertrap (operated at
212 205 K) a bare steel trap ($\geq 24 \text{ K}$) and a charcoal trap ($\geq 10 \text{ K}$). The cold trap unit is controlled

213 by a Lakeshore 336 Controller (Cryotronics). This module is pumped by an ion pump (Agilent,
214 Vacion 40 plus Starcell).

215
216 The performance of the bare cold trap unit for He, Ne, Ar-separation was calibrated using the
217 Residual Gas Analyser (Hiden HAL/3F PIC). Neon is quantitatively adsorbed on the bare trap at
218 24 K (>99.9985 % is adsorbed at 24 K; Fig. 2), in equilibrium about 60% of the helium is adsorbed
219 at 24 K. We use this to separate helium from neon. Helium is removed (distilled-off in
220 disequilibrium) either to the ion pump or the 10 K charcoal head, the latter if the He is to be
221 retained for analysis. Neon is fully released from the bare trap at 80 K, at this temperature argon
222 is quantitatively retained on the bare trap, permitting quantitative separation of the two gases
223 (Fig. 2).

224 Besides its functionality to separate noble gases from each other the bare trap serves as coldtrap
225 during Ne-analysis (held at 80 K) and replaces a liquid nitrogen cooled trap, which would
226 otherwise customarily be used for this purpose. The latter may introduce intensity fluctuations
227 during analysis due to changing coolant level, which we avoid with our setup. The last
228 pneumatically actuated valve before the Helix-Plus MCMS serves as inlet valve, the manual valve
229 of the Helix-Plus MCMS is permanently open.



230
231 *Fig. 2: Desorption curves of Ne and Ar on the stainless-steel cold trap measured with the Hiden*
232 *Quadrupole. The uncertainties of the argon determinations at low fractions released are due to a*
233 *significant Ar-background of the quadrupole (e.g., measurement at 100 K was just 5% higher than*
234 *the background).*

235 **2.3 Automation**

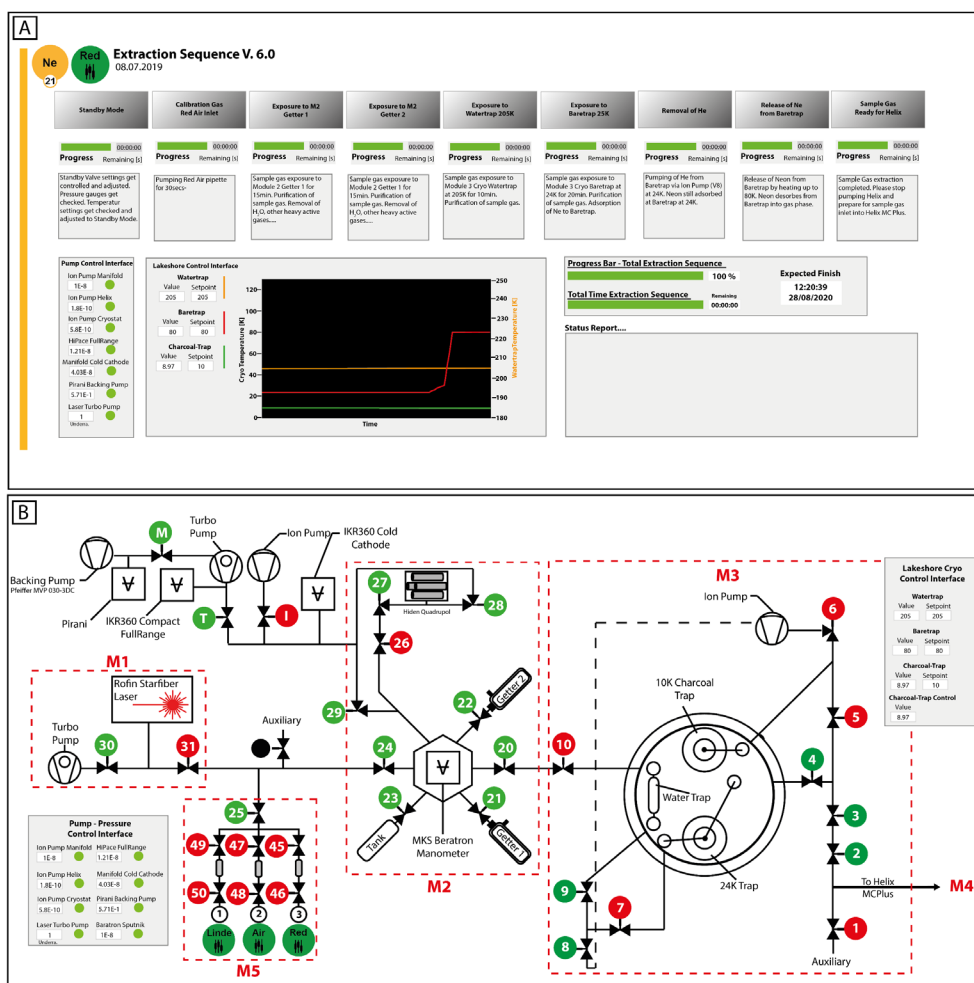
236 The extraction and purification line can either be operated manually, via a switchboard for the
237 pneumatic valves and the components' original controllers, or automatically via LabView. Manual
238 operation is mainly used for development of analytical routines, automatic operation generally

239 for sample and calibration-gas analysis. Automatic operation liberates the operator from
240 conducting necessarily repetitive tasks, thus helps to prevent mistakes and inconsistencies from
241 oversight or negligence; it allows to conduct gas purification and separation under precisely
242 identical conditions. The latter is also assisted by avoiding liquid coolants, which commonly are
243 affected by variable coolant levels (unless automatically filled with a suitably precise system or an
244 experienced and conscientious operator). Currently the laser system is operated manually (due
245 to safety regulations); all subsequent steps - until admission of the gas to the mass spectrometer
246 - are automated utilizing LabView (Version 2018) in a Windows 10 environment. The mass
247 spectrometry analysis of the purified gas is conducted with Qtegra (Thermo Fisher Scientific).

248 Valve control electronics were developed and implemented in-house, including digital
249 input/output modules (I/O modules from National Instruments) and RS-232 communication.
250 Main devices such as, SAES getter control, Lakeshore Cryo-Controller, turbo and ion pumps
251 offered already LabView compatible Sub-VI's (Virtual Instrument, **program codes**), which were
252 implemented into the operation VI. The Agilent Ion Pump Control connection via the computer
253 interfaces were written/developed in-house.

254 The gauges and controllers of the Turbo pumps (Pfeiffer) and Ion pumps (Agilent) are monitored
255 via the operation VI. Automatic safety protocols are implemented to protect the extraction line
256 and equipment against sudden pressure increases. Temperature setting and monitoring of the
257 three cold traps (Janis Cryostat) is performed by the Lakeshore 336 controller, which in turn is
258 controlled via the operation VI.

259 LabView computing of the extraction sequence/protocol was programmed in single commands
260 and steps, joined into command sequences connected in series as sub-VIs for each extraction
261 protocol (various noble gases and sources of samples or calibration gas). Pressure and
262 temperature control sequences are programmed in continuous loop to ensure stability and safety
263 during operation. For handling, a structured user interface was designed (Fig. 3), which provides
264 the user with information about all parameters, total duration, and additionally logs every
265 extraction step.



266

267 Fig. 3: Screenshots of the operating VIs of the Cologne Noble Gas Helix MCPlus. (A) The Neon VI
 268 informs the user in real time about current data, such as pressure and temperature, as well as about
 269 the current status of the preparation (B) Valve circuit overview.

270 3. Analytical Procedure

271 Quartz samples are cleaned using standard procedures using dilute HF as etchant (Kohl and
 272 Nishiizumi, 1992). Up to 600 mg of quartz are loaded into tungsten-cups and covered with a
 273 tungsten-lid, the latter has a small hole to facilitate gas release. When opening the laser furnace
 274 for re-loading, the furnace is vented and purged with a continuous flow of pure nitrogen. In normal
 275 operation, after the initial installation and bake-out, the internal parts of the furnace are never
 276 again exposed to air. The tungsten cups and lids remain in the nitrogen atmosphere during sample
 277 (re-)loading. Cups are emptied with a suction micropicker (Micropicker MPC100, VU Amsterdam)
 278 while seated in the revolver, and weighed samples are transferred from the glass vials into the
 279 cup through a miniature metal funnel (glass funnels produced undesirable static effects). After
 280 reloading, the sample revolver is heated by firing the laser on an empty cup; pressure $<5 \cdot 10^{-9}$
 281 mbar is usually achieved after pumping overnight. During this clean-up, and during subsequent
 282 analyses, the temperature of adjacent cups does not exceed 156.6 °C (verified with Indium wire).

283 Cosmogenic Ne is extracted from quartz by heating the sample with a defocused laser beam at
284 100 W for 15 min; at these settings, the cup-insides reach ~ 1200 °C. This temperature allows
285 reliable extraction of cosmogenic neon (Vermeesch et al., 2015). After heating the furnace, it is
286 allowed to cool for five minutes before the sample is expanded to the clean-up module.

287 For calibrations, the calibration gas is expanded for 30 sec into the pipette, the pipette volume is
288 then expanded into the clean-up volume. After this step, purification is identical for sample and
289 calibration gases. The pipetting of calibration gas, and the purification of sample and calibration
290 gases, is fully automatized.

291 Reactive gases are removed by sequential exposure to two metal getters (SAES NP50); the first is
292 operated hot, the other at room temperature. The gas is exposed to each for 15 min. Subsequently
293 the gas is exposed to the water trap at 205 K for 10 min. The remaining inert gases are exposed to
294 the bare-metal trap at 24 K for 20 min, which is then pumped for 5 min to remove helium from
295 the sample gas. The trap is then isolated and heated to 80 K, followed by five-minutes holding time
296 for re-equilibration. Neon is quantitatively released, and argon is quantitatively retained on the
297 trap. **Subsequently**, Ne gas is expanded into the Helix MCMS for analysis. The bare trap at 80 K
298 remains connected to the mass spectrometer during analysis, for pumping of CO₂ and Ar evolving
299 from the mass spectrometer.

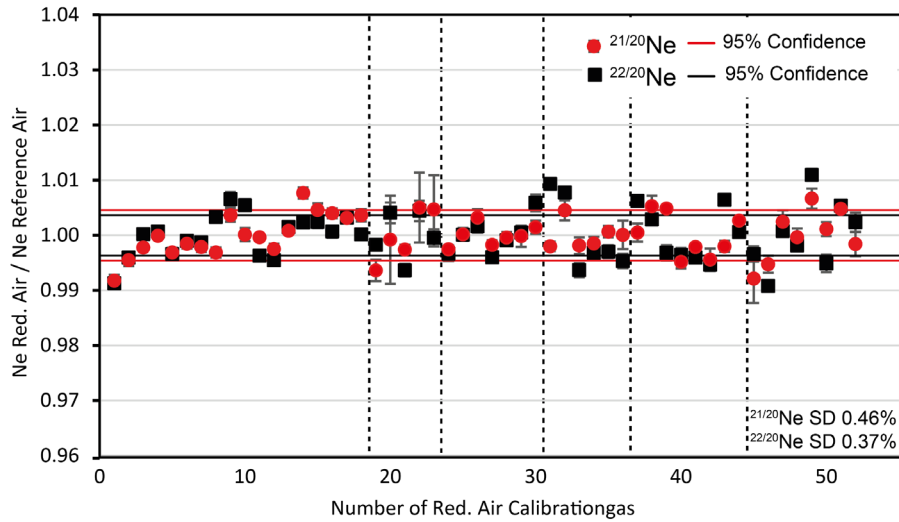
300 The configuration of the Helix is described above. For maximum sensitivity and precision for
301 abundance determination (Wielandt and Storey, 2019), we use the widest (0.25 mm) source slit
302 for neon analysis. We run the source at an electron energy of 115 eV, trap current of 200 μ A and
303 an acceleration voltage of 9.9 kV.

304 ²⁰Ne is measured on the high-resolution L1 Faraday cup (fitted with 10¹³ Ω pre-amplifier), fully
305 resolved from ⁴⁰Ar²⁺ and from molecular interferences such as HF⁺, H₂¹⁸O⁺. ²¹Ne is measured
306 off-centre on the high-resolution L1 multiplier, at a position that is free from interference from
307 ²⁰NeH⁺. ²²Ne is measured at peak centre on the H1 Faraday cup (fitted with 10¹³ Ω pre-amplifier);
308 interference from CO₂²⁺ is corrected via monitoring of the double/single-charged ratio of CO₂
309 in-between samples and measurement of CO₂ during sample analysis, which we found to be stable
310 at 0.0437 ± 0.001 for our system throughout the period for which the data we report here were
311 obtained. The corresponding corrections of ²²Ne intensities are < 0.3 % for one shot of 'RedAir'
312 calibration gas (~ 17 fmol ²²Ne). The uncertainties of the correction are ~ 2 %, which add $< 0.006\%$
313 **uncertainty to the intensity determinations for 'RedAir'. These values scale linearly for smaller or**
314 **larger amounts of ²²Ne as found in samples.** CO₂⁺ is measured on the Faraday cup of the Axial
315 collector (fitted with 10¹³ Ω pre-amplifier). We refrain from analysing the larger Neon-beams
316 (²²Ne, ²⁰Ne) on the multipliers, since we found that they are a significant source of CO₂ upon being
317 hit by beams larger than those typical for ²¹Ne signals (for analysing blanks, however, we use a

318 multiplier for ^{20}Ne and ^{22}Ne). Besides, the Faraday cups have a superior linearity and stability over
319 time (Wielandt and Storey, 2019). The mass spectrometer sensitivity, mass-discrimination and
320 multiplier vs. Faraday gain is calibrated with 'RedAir', which is measured at least once a day during
321 sample runs. Each batch of samples includes at least one measurement of ~ 100 mg CREU-1
322 (Vermeesch et al., 2015) to monitor the performance of the extraction and purification system.
323 We are in the process of producing a new intercomparison material to replace CREU-1, whose
324 supplies are limited and eventually will run too low for regular use.

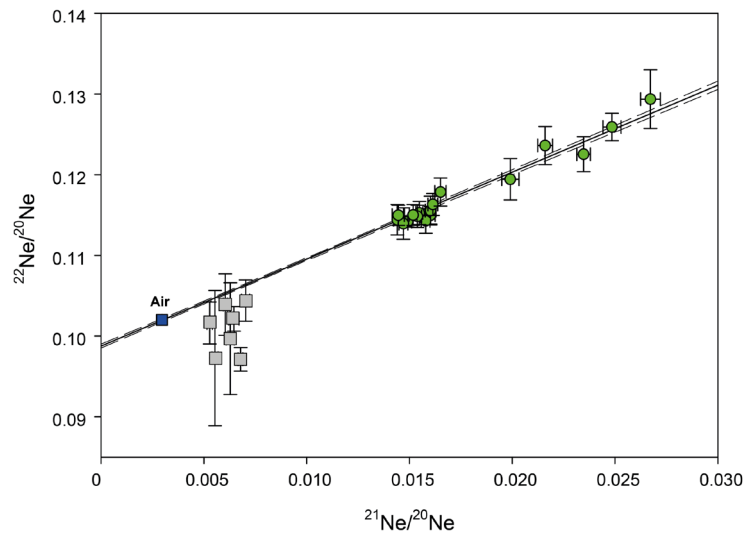
325 **4. Performance**

326 The within-run reproducibility of Neon-isotope ratios as determined for calibration gas ('RedAir',
327 ~ 17 fmol atmospheric Ne) is similar for $^{21}\text{Ne}/^{20}\text{Ne}$ and $^{22}\text{Ne}/^{20}\text{Ne}$ ratios, with 0.46 % and 0.37 %
328 ($\pm 1\sigma$, $n=52$), respectively. This dispersion is larger than the uncertainty of individual
329 measurements (Fig. 4); this feature, and the values for dispersion, are similar to those reported
330 for other Helix Plus instruments (Honda et al., 2015; Wielandt and Storey, 2019). **The second**
331 **measurement period, with the increased uncertainties of the $^{21}\text{Ne}/^{20}\text{Ne}$ ratios, was performed**
332 **after an extended period of development work for other noble gas isotopes.** We use the means
333 and the uncertainty of the means of calibrations within runs to calibrate the measurements
334 samples, i.e., propagate the observed dispersion in calculations of the abundance of cosmogenic
335 ^{21}Ne in samples. **Derived $^{21}/^{20}\text{Ne}$ and $^{22}/^{20}\text{Ne}$ ratios of 22 aliquots of CREU-1, including five power**
336 **step extractions (Table 1), reveal a spallation line of 1.078 ± 0.022 ($\pm 2\sigma$), which is**
337 **indistinguishable from the published value of 1.108 ± 0.014 ($\pm 2\sigma$; Vermeesch et al., 2015, Fig. 5).**
338 The calculated cosmogenic ^{21}Ne abundances from 22 aliquots of CREU-1 (Table 1) all agree within
339 2σ with their arithmetic mean ($348 \pm 10 * 10^6$ atoms/g; $\pm 2\sigma$); thus, we may calculate an error-
340 weighted mean: $348 \pm 2 * 10^6$ atoms/g ($\pm 2\sigma$), which is indistinguishable from the published value
341 ($348 \pm 10 * 10^6$ atoms/g; Vermeesch et al., 2015, see Fig. 6). We conclude that the reproducibility
342 and accuracy of the current set up at the University of Cologne for determining cosmogenic ^{21}Ne
343 in quartz is similar to or better than those reported for other laboratories worldwide (Vermeesch
344 et al., 2015, Fig. 6; Farley et al., 2020; Ma et al., 2015).



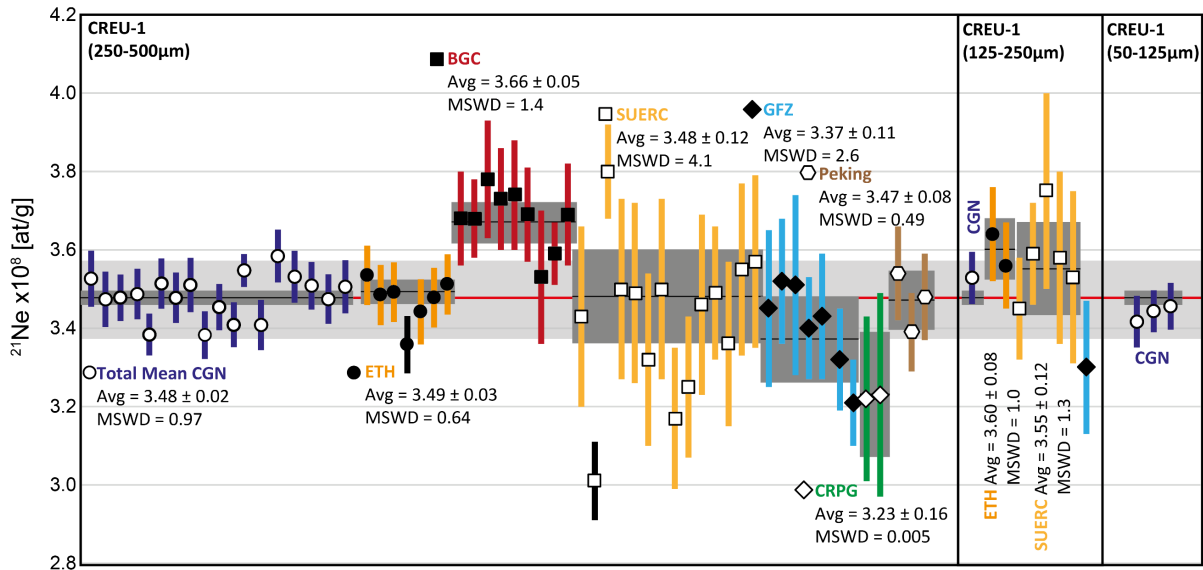
345

346 *Fig. 4: Reproducibility of standard gas ‘RedAir’ measurements for sample runs, during the period*
 347 *between March 2020 and December 2020. Isotopic ratios are normalized to air for each run (mean*
 348 *of isotope ratios obtained in run/atmospheric ratio). Stippled black lines delineate individual runs.*
 349 *Error bars on individual data points are $\pm 1\sigma$. Symbol size is commonly larger than the corresponding*
 350 *error bars, which may therefore be hidden.*



351

352 *Fig. 5: Neon-three-isotope plot for CREU-1 intercomparison material measured in Cologne. Error*
 353 *bars are $\pm 1\sigma$. The cloud of green symbols displays single-step CREU extractions (100 W-15 min), the*
 354 *green dots to the right of the cluster are the initial heating steps of stepwise extractions (at varying*
 355 *laser output), grey rectangles are the subsequent steps that invariably had low abundance; for*
 356 *details see Table 1. Data of samples depicted in green are included in the regression calculation; data*
 357 *of the grey rectangles are excluded. The slope of the regression of the data (forced through air) is*
 358 *1.078 ± 0.022 ($\pm 2\sigma$), which is indistinguishable from the published value of 1.108 ± 0.014 ($\pm 2\sigma$;*
 359 *Vermeesch et al., 2015). The dotted line denotes the 95% confidence interval.*



360

361 Fig. 6: Compilation of CREU-1 ^{21}Ne concentrations ($\pm 2\sigma$ uncertainties) measured at Cologne (CGN),
 362 compared to reported ^{21}Ne concentrations from interlaboratory comparison from Vermeesch et al.
 363 (2015) and data from the Peking noble gas lab from Ma et al. (2015). Black bars were considered
 364 outliers by the original authors and not used for calculation of averages (Vermeesch et al., 2015).
 365 The data is divided into three sections, each for a different CREU-1 grain-size analysed. The average
 366 ^{21}Ne concentration for CREU-1 of $3.48 \pm 10 \cdot 10^8$ at/g reported by Vermeesch et al. (2015) is marked
 367 as light-grey band and a red line for the mean. Lab-individual error-weighted means are displayed
 368 as black lines with their respective uncertainty in dark grey. The average obtained for CREU-1 at
 369 Cologne (all grain-sizes, $n=22$) is $3.48 \pm 0.02 \cdot 10^8$ at/g ($\pm 2 \sigma$; error-weighted standard deviation).
 370 The MSWD values (Mean Square of the Weighted Deviates ('reduced Chi-square', McIntyre et al.
 371 (1966)) are reported for all individual laboratory-means (Vermeesch et al., 2015; this study). CGN =
 372 University of Cologne, ETH = Eidgenössische Technische Hochschule Zürich, BGC = Berkeley
 373 Geochronology Center, SUERC = Scottish Universities Environmental Research Centre Glasgow, CRPG
 374 = Centre de Recherches Pétrographiques et Géochimiques Nancy, GFZ = Deutsches
 375 GeoForschungsZentrum Potsdam.

376 Table 1: CREU Data

Sample ID	Mass [g]	Extraction Power [W]	^{20}Ne		21/20		22/20		$^{21}\text{Ne}^*$ [10 ⁶ at/g]
			[10 ⁹ at/g]						
01_CREU1 250-500µm	0.0997	100	30.97 ± 0.15		0.01434 ± 0.00014		0.11381 ± 0.00129		352.7 ± 3.6
02_CREU1 250-500µm	0.0993	100	29.81 ± 0.24		0.01461 ± 0.00015		0.11415 ± 0.00129		347.4 ± 3.5
03_CREU1 50-125µm	0.1038	100	24.89 ± 0.15		0.01669 ± 0.00012		0.11646 ± 0.00170		341.7 ± 3.3
04_CREU1 50-125µm	0.1319	100	25.73 ± 0.20		0.01634 ± 0.00018		0.11727 ± 0.00089		344.4 ± 2.7
05_CREU1 50-125µm	0.1179	100	24.86 ± 0.17		0.01686 ± 0.00017		0.11614 ± 0.00130		345.6 ± 3.0

06_CREU1												
125-250µm	0.1078	100	27.00	± 0.35	0.01603	± 0.00022	0.11499	± 0.00110	352.9	± 3.3		
07_CREU1												
250-500µm	0.1210	100	29.13	± 0.36	0.01490	± 0.00021	0.11417	± 0.00065	347.8	± 3.0		
08_CREU1												
250-500µm	0.1105	100	30.46	± 0.25	0.01441	± 0.00018	0.11443	± 0.00189	348.7	± 3.2		
09_CREU1												
250-500µm	0.1312	100	26.37	± 0.32	0.01579	± 0.00021	0.11428	± 0.00153	338.4	± 2.7		
10_CREU1												
250-500µm	0.1128	100	29.92	± 0.40	0.01470	± 0.00022	0.11395	± 0.00195	351.4	± 3.2		
11_CREU1												
250-500µm	0.1113	100	26.60	± 0.33	0.01603	± 0.00026	0.11556	± 0.00179	347.8	± 3.2		
12_CREU1												
250-500µm	0.1053	100	30.56	± 0.36	0.01445	± 0.00030	0.11498	± 0.00125	351.1	± 3.5		
13_CREU1												
250-500µm	0.1125	100	27.01	± 0.24	0.01548	± 0.00017	0.11526	± 0.00143	338.3	± 3.0		
14_CREU1												
250-500µm	0.1210	100	26.21	± 0.30	0.01614	± 0.00024	0.11632	± 0.00137	345.4	± 3.0		
15_CREU1												
250-500µm	0.1252	100	25.16	± 0.19	0.01651	± 0.00027	0.11786	± 0.00174	340.9	± 2.9		
16_CREU1												
250-500µm	0.2063	100	28.54	± 0.33	0.01539	± 0.00020	0.11485	± 0.00137	354.8	± 2.1		
17_CREU1												
250-500µm	0.1077	100	27.90	± 0.30	0.01518	± 0.00019	0.11502	± 0.00129	340.9	± 3.2		
18_CREU1												
250-500µm	0.1126	30	16.44	± 0.16	0.02160	± 0.00036	0.12362	± 0.00236				
	0.1126	50	8.61	± 0.08	0.00628	± 0.00019	0.09968	± 0.00692				
	0.1126	70	5.71	± 0.05	0.00528	± 0.00013	0.10162	± 0.00260				
	0.1126	100	3.92	± 0.05	0.00554	± 0.00015	0.09727	± 0.00838	358.5	± 3.4		
19_CREU1												
250-500µm	0.1111	24	11.96	± 0.17	0.02672	± 0.00048	0.12936	± 0.00364				
	0.1111	100	18.06	± 0.23	0.00678	± 0.00012	0.09711	± 0.00146	353.2	± 3.3		
20_CREU1												
250-500µm	0.1301	24	14.27	± 0.12	0.02347	± 0.00033	0.12255	± 0.00217				
	0.1301	100	16.51	± 0.18	0.00646	± 0.00025	0.10213	± 0.00152	350.9	± 3.0		
21_CREU1												
250-500µm	0.1180	30	13.11	± 0.15	0.02485	± 0.00044	0.12592	± 0.00170				
	0.1180	100	14.79	± 0.09	0.00703	± 0.00020	0.10440	± 0.00256	347.5	± 3.2		
22_CREU1												
250-500µm	0.1075	50	18.42	± 0.12	0.01991	± 0.00042	0.11944	± 0.00256				
	0.1075	100	12.35	± 0.11	0.00604	± 0.00010	0.10391	± 0.00381	350.6	± 3.4		

377

378 **Conclusion**

379 The performance of the set-up for Neon-isotope measurements in the new noble gas laboratory
380 at the University Cologne permits state-of-the art analysis of cosmogenic neon. We now regularly
381 perform analysis of samples for cosmogenic neon for our running projects; and are open to new
382 scientific cooperations.

383 **Author contribution:**

384 TJD, BR, AV **development of the Cologne** noble gas system. TJD, BR performance experiments and
385 tests. BR, TJD manuscript writing.

386 **Data Availability:**

387 The authors confirm that the data supporting the findings of this study are available within the
388 article.

389 **Acknowledgements:**

390 The equipment for the noble gas mass spectrometry laboratory described in this paper was
391 funded by Deutsche Forschungsgemeinschaft (DFG) - project number 259990027 to TJD. The
392 performance test was conducted and funded in the framework of the Collaborative Research
393 Center 1211 – Earth Evolution at the Dry Limit, Deutsche Forschungsgemeinschaft (DFG) - project
394 number 268236062 – SFB 1211. Special thanks go to Dave Wanless for patient training and
395 continuing support in mastering ‘Aura’.

396 **Declaration of interest**

397 The authors declare that the research was conducted in the absence of any commercial or financial
398 relationships that could be construed as a potential conflict of interest.

399 **References**

400 Binnie, S., Reicherter, K., Victor, P., González, G., Binnie, A., Niemann, K., Stuart, F., Lenting, C.,
401 Heinze, S., Freeman, S., and Dunai, T. J.: The origins and implications of paleochannels in hyperarid,
402 tectonically active regions: The northern Atacama Desert, Chile, *Global and Planetary Change*, 185,
403 103083, 2020.

404

405 Dunai, T. J.: *Cosmogenic Nuclides: Principles, concepts and applications in the Earth surface sciences*,
406 Cambridge University Press 2010.

407

408 Dunai, T. J., Lopez, G. A. G., and Juez-Larre, J.: Oligocene-Miocene age of aridity in the Atacama
409 Desert revealed by exposure dating of erosion-sensitive landforms, *Geology*, 33, 321-324,
410 10.1130/g21184.1, 2005.

411

412 Eberhardt, P., Eugster, O., and Marti, K.: A redetermination of the isotopic composition of
413 atmospheric neon, *Zeitschrift für Naturforschung*, 20a, 623-624, 1965.

414

415 Espanon, V. R., Honda, M., and Chivas, A. R.: Cosmogenic ³He and ²¹Ne surface exposure dating of
416 young basalts from Southern Mendoza, Argentina, *Quaternary Geochronology*, 19, 76-86, 2014.

417

418 Farley, K., Treffkorn, J., and Hamilton, D.: Isobar-free neon isotope measurements of flux-fused
419 potential reference minerals on a Helix-MC-Plus10K mass spectrometer, *Chemical Geology*, 537,
420 119487, 2020.

421

422 Gillen, D., Honda, M., Chivas, A. R., Yatsevich, I., Patterson, D. B., and Carr, P. F.: Cosmogenic ²¹Ne
423 exposure dating of young basaltic lava flows from the Newer Volcanic Province, western Victoria,
424 Australia, *Quaternary Geochronology*, 5, 1-9, 2010.

425

426 Györe, D., Tait, A., Hamilton, D., and Stuart, F. M.: The formation of NeH⁺ in static vacuum mass
427 spectrometers and re-determination of ²¹Ne/²⁰Ne of air, *Geochimica et Cosmochimica Acta*, 263, 1-
428 12, 2019.
429

430 Honda, M., Zhang, X., Phillips, D., Hamilton, D., Deerberg, M., and Schwieters, J. B.: Redetermination
431 of the ²¹Ne relative abundance of the atmosphere, using a high resolution, multi-collector noble gas
432 mass spectrometer (HELIX-MC Plus), *International Journal of Mass Spectrometry*, 387, 1-7, 2015.
433

434 Kohl, C. and Nishiizumi, K.: Chemical isolation of quartz for measurement of in-situ-produced
435 cosmogenic nuclides, *Geochimica et Cosmochimica Acta*, 56, 3583-3587, 1992.
436

437 Ma, Y., Wu, Y., Li, D., and Zheng, D.: Analytical procedure of neon measurements on GV 5400 noble
438 gas mass spectrometer and its evaluation by quartz standard CREU-1, *International Journal of Mass
439 Spectrometry*, 380, 26-33, 2015.
440

441 Ma, Y., Wu, Y., Li, D., Zheng, D., Zheng, W., Zhang, H., Pang, J., and Wang, Y.: Erosion rate in the
442 Shapotou area, northwestern China, constrained by in situ-produced cosmogenic ²¹Ne in long-
443 exposed erosional surfaces, *Quaternary Geochronology*, 31, 3-11, 2016.
444

445 McIntyre, G., Brooks, C., Compston, W., and Turek, A.: The statistical assessment of Rb-Sr isochrons,
446 *Journal of Geophysical Research*, 71, 5459-5468, 1966.
447

448 McPhillips, D., Hoke, G. D., Liu-Zeng, J., Bierman, P. R., Rood, D. H., and Niedermann, S.: Dating the
449 incision of the Yangtze River gorge at the First Bend using three-nuclide burial ages, *Geophysical
450 Research Letters*, 43, 101-110, 2016.
451

452 Niedermann, S.: Cosmic-ray-produced noble gases in terrestrial rocks: dating tools for surface
453 processes, *Reviews in Mineralogy and Geochemistry*, 47, 731-784, 2002.
454

455 Niedermann, S., Graf, T., Kim, J., Kohl, C., Marti, K., and Nishiizumi, K.: Cosmic-ray-produced ²¹Ne in
456 terrestrial quartz: the neon inventory of Sierra Nevada quartz separates, *Earth and Planetary Science
457 Letters*, 125, 341-355, 1994.
458

459 Ritter, B., Stuart, F. M., Binnie, S. A., Gerdes, A., Wennrich, V., and Dunai, T. J.: Neogene fluvial
460 landscape evolution in the hyperarid core of the Atacama Desert, *Scientific Reports*, 8, 13952,
461 10.1038/s41598-018-32339-9, 2018.
462

463 Saxton, J.: The ²¹Ne/²⁰Ne ratio of atmospheric neon, *Journal of Analytical Atomic Spectrometry*,
464 35, 943-952, 2020.
465

466 Vermeesch, P., Balco, G., Blard, P. H., Dunai, T. J., Kober, F., Niedermann, S., Shuster, D. L., Strasky, S.,
467 Stuart, F. M., Wieler, R., and Zimmermann, L.: Interlaboratory comparison of cosmogenic Ne-21 in
468 quartz, *Quaternary Geochronology*, 26, 20-28, 10.1016/j.quageo.2012.11.009, 2015.
469

470 Wielandt, D. and Storey, M.: A new high precision determination of the atmospheric ^{21}Ne
471 abundance, *Journal of Analytical Atomic Spectrometry*, 34, 535-549, 2019.

472